Journal of Modern Optics
Vol. 56, Nos. 18–19, 20 October–10 November 2009, 2029–2033

Estimation of the spatial bandwidth of an optical parametric amplifier with plane-wave pump

Michael Vasilyev[a]*, Nikolai Stelmakh[a] and Prem Kumar[b]

[a]*Department of Electrical Engineering, University of Texas at Arlington, 416 Yates St., Arlington, TX 76019, USA;* [b]*Center for Photonic Communication and Computing, EECS Department, Northwestern University, 2145 Sheridan Rd., Evanston, IL 60208, USA*

(*Received 23 March 2009; final version received 1 July 2009*)

We analyze the spatial-frequency dependence of the gain of phase-insensitive and phase-sensitive optical parametric amplifiers with plane-wave pumping. We discuss the dependence of their spatial bandwidths on pump power and crystal length, L, and observe that the well-known $(k_s/L)^{1/2}$ approximation of spatial bandwidth is not very accurate (here k_s is the signal beam's wavevector magnitude). We derive an alternative approximation that is highly accurate at large gains and moderately accurate at low gains. The differences between the phase-insensitive and phase-sensitive amplifier bandwidths are shown to be insignificant for gains above several dB. Maximum phase-sensitive gain and bandwidth are realized by imposing an optimum phase profile onto the input signal's spatial spectrum, which has nearly parabolic shape with added series of $\pi/2$ phase discontinuities at spatial frequencies outside the main bandwidth of the amplifier. We show that, apart from the discontinuities, such a profile can be closely approximated by placing the image plane into the middle of the nonlinear crystal (converging input beam). The phase discontinuities contribute an additional narrow component to the point-spread function of the phase-sensitive amplifier.

Keywords: optical parametric amplifiers; phase-sensitive amplifiers; image amplification

Spatially broadband optical parametric amplifiers (OPAs) have gained considerable attention recently in the context of amplification and time gating of images [1], noiseless amplification of images [2,3], and improvement of sensitivity and resolution of coherent laser radars (LADARs) [4], with recent research activity nicely summarized in [1,5]. In the practical design of such amplifiers, some simple analytical estimates are required for the OPA spatial bandwidth and, particularly, its scaling (if any) with nonlinear crystal length and pump power. A well-known estimate for spatial bandwidth is $(k_s/L)^{1/2}$, which was derived in [6] and is commonly used in *qualitative* discussions [1–4]. However, it is not clear how *quantitatively* accurate this estimate is and whether it is really useful in predicting the noticeable image quality degradation or spread of spatial noise correlations in OPAs.

In this paper, we compute the 3 dB spatial bandwidths of phase-insensitive and phase-sensitive OPAs with plane-wave pump, compare them with the above analytical estimate, and derive a more accurate approximation. We also investigate the impact of sub-optimal signal phase on the spatial bandwidth and point-spread function of the phase-sensitive OPAs.

Let us start by writing equations relating the input and output electric fields in an OPA of length L. In paraxial approximation the output of the OPA with plane-wave pump is given by

$$\tilde{E}_s(\boldsymbol{q}, L) = \mu(q)\tilde{E}_s(\boldsymbol{q}, 0) + \nu(q)\tilde{E}_i^*(-\boldsymbol{q}, 0), \tag{1}$$

where

$$\begin{aligned}\mu(q) &= \left(\cosh\gamma L - \frac{i\Delta k_{\mathrm{eff}}}{2\gamma}\sinh\gamma L\right) \\ &\quad\times \exp\left(i\frac{\Delta k_{\mathrm{eff}}}{2}L\right)\exp\left(-i\frac{q^2}{2k_s}L\right), \\ \nu(q) &= i\frac{\kappa_s}{\gamma}\sinh\gamma L \times \exp\left(i\frac{\Delta k_{\mathrm{eff}}}{2}L\right)\exp\left(-i\frac{q^2}{2k_s}L\right),\end{aligned} \tag{2}$$

the effective wavevector mismatch is

$$\begin{aligned}\Delta k_{\mathrm{eff}} &= k_p - k_s - k_i + \frac{q^2}{2}\left(\frac{1}{k_s} + \frac{1}{k_i}\right), \\ &= \Delta k + \frac{q^2}{2}\left(\frac{1}{k_s} + \frac{1}{k_i}\right),\end{aligned} \tag{3}$$

*Corresponding author. Email: vasilyev@uta.edu

ISSN 0950–0340 print/ISSN 1362–3044 online

DOI: 10.1080/09500340903156814
http://www.informaworld.com

and the parametric gain coefficient is

$$\gamma = \left(\kappa^2 - \Delta k_{\mathrm{eff}}^2/4\right)^{1/2}, \tag{4}$$

with

$$\kappa^2 = \kappa_{\mathrm{s}}\kappa_{\mathrm{i}} = \frac{\omega_{\mathrm{s}}\omega_{\mathrm{i}} d_{\mathrm{eff}}^2 I_{\mathrm{p}}}{2\varepsilon_0 n_{\mathrm{s}} n_{\mathrm{i}} n_{\mathrm{p}} c^3}, \qquad \kappa_{\mathrm{s}} = \frac{\omega_{\mathrm{s}} d_{\mathrm{eff}}}{n_{\mathrm{s}} c}|E_{\mathrm{p}}|, \tag{5}$$

and initial phase of the pump field E_{p} is assumed to be zero [6]. We use subscripts 's', 'i', and 'p' for the signal, idler, and pump waves, respectively. Optical frequency is denoted by ω, refractive index by n, effective nonlinear coefficient by d_{eff}, intensity by I, and spatial frequency (rad mm^{-1}) by $\boldsymbol{q}$. We utilize tildes on top of electric field symbols to show signals in the spatial-frequency domain. For the degenerate case the product of the exponentials in Equations (2), containing the effective mismatch and diffraction phase terms, becomes simply $\exp(\mathrm{i}\Delta kL/2)$. This is also approximately true for the non-degenerate case (if $k_{\mathrm{s}} \approx k_i$, which we will assume through the rest of this paper). The optimum signal phase for maximum phase-sensitive gain is given by

$$\theta_{\mathrm{s}}^{\mathrm{opt}} = \frac{\pi}{4} + \frac{1}{2}\tan^{-1}\left[\frac{\Delta k_{\mathrm{eff}}}{2\gamma}\tanh\gamma L\right] + \frac{1}{2}\arg\left[\frac{\kappa_{\mathrm{s}}}{\gamma}\sinh\gamma L\right]. \tag{6}$$

The phase-insensitive-amplifier (PIA) gain is given by

$$G_{\mathrm{PIA}} = |\mu(q)|^2 = 1 + |\nu(q)|^2 = 1 + \frac{\sinh^2(\kappa L(1-r^2)^{1/2})}{1-r^2} \tag{7}$$

$$= 1 + \frac{\sinh^2\left[\kappa L\left[1 - \left(\pi\lambda_{\mathrm{s}} f^2/n_{\mathrm{s}}\kappa\right)^2\right]^{1/2}\right]}{1 - \left(\pi\lambda_{\mathrm{s}} f^2/n_{\mathrm{s}}\kappa\right)^2} \quad (\text{for } \Delta k = 0), \tag{7a}$$

where we have introduced spatial frequency in mm^{-1} $f = q/(2\pi)$ and phase mismatch factor

$$r = \frac{\Delta k_{\mathrm{eff}}}{2\kappa} = \frac{\Delta k}{2\kappa} + \frac{q^2}{2k_{\mathrm{s}}\kappa} = \frac{\Delta k}{2\kappa} + \frac{\pi\lambda_{\mathrm{s}} f^2}{n_{\mathrm{s}}\kappa}. \tag{8}$$

The PIA gain is plotted in Figure 1 for the parameters of our experimental paper [3] (*a*) and for the parameters of interest in our current experiments (*b*), assuming $\Delta k = 0$. Figure 1 also shows the optimum signal phase (6) (normalized by π) versus spatial frequency. For $r \geq 1$, the sinh function in Equation (7) becomes the i sin function, i.e.

$$G_{\mathrm{PIA}} = |\mu(q)|^2 = 1 + |\nu(q)|^2 = 1 + \left[\kappa L \times \mathrm{sinc}\left(\kappa L (r^2-1)^{1/2}\right)\right]^2, \tag{9}$$

and $G_{\mathrm{PIA}} = 1 + (\kappa L)^2$ for $r = 1$. For $\Delta k = 0$, the first zero of the sinc function [which is also the first zero of $\nu(q)$] takes place at

$$f_0 = \left[\frac{k_{\mathrm{s}}^2}{4\pi^2}\left(\frac{\kappa^2}{\pi^2} + \frac{1}{L^2}\right)\right]^{1/4}, \tag{10}$$

which can be approximated as

$$f_0 \approx \left(\frac{k_{\mathrm{s}}}{2\pi L}\right)^{1/2} \quad \text{for } \kappa L \ll 1, \tag{11}$$

$$f_0 \approx \frac{1}{\pi}\left(\frac{k_{\mathrm{s}}\kappa}{2}\right)^{1/2} \quad \text{for } \kappa L \gg 1. \tag{12}$$

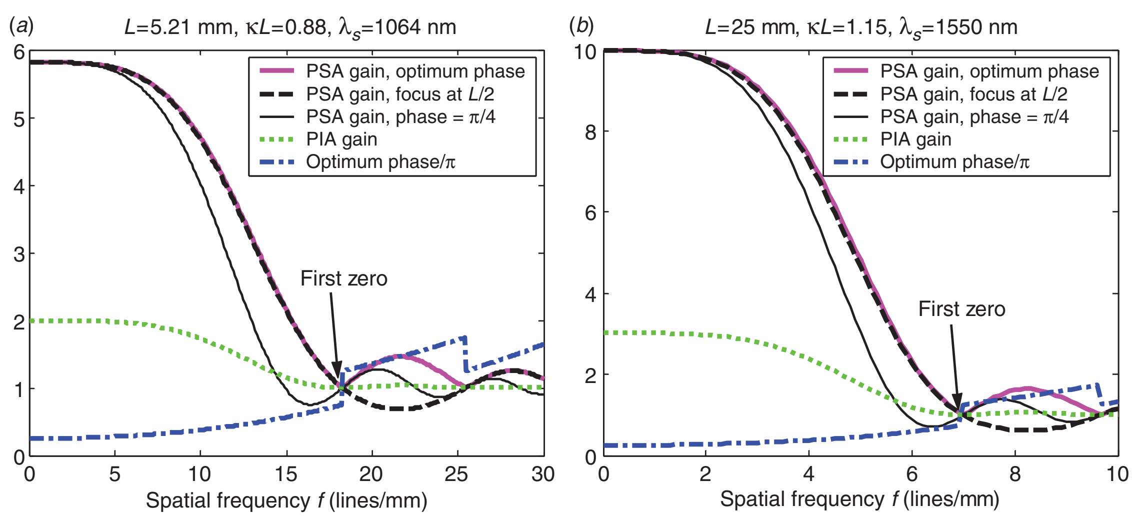

Figure 1. OPA gains (linear scale) versus spatial frequency $f = q/(2\pi)$ for parameters of our paper [3] (*a*) and parameters of current experiments (*b*), assuming $\Delta k = 0$. Optimum signal phase $\theta_{\mathrm{s}}^{\mathrm{opt}}$ maximizing the PSA gain is also shown. Arrow indicates the location of the first zero of the $\nu(2\pi f)$ function. (The color version of this figure is included in the online version of the journal.)

Equation (11) represents the well-known $q \sim (k_s/L)^{1/2}$ estimate for the spatial bandwidth with $L^{-1/2}$ scaling. The estimates given by Equations (10)–(12) are plotted in Figures 2 and 3 and compared to the actual 3 dB bandwidth of PIA gain (7).

An alternative way to estimate the 3 dB bandwidth for large pump powers (i.e. large κ) is to note that sinh becomes an exponent at high gains, i.e.

$$G_{\mathrm{PIA}} \approx \frac{\exp[2\kappa L(1-r^2)^{1/2}]}{4(1-r^2)} \approx \frac{1}{4}\exp(2\kappa L)\exp(-\kappa L r^2), \tag{13}$$

and, for $\Delta k = 0$, at 3 dB bandwidth f_c we have

$$\exp(-\kappa L r^2) = \tfrac{1}{2}, \tag{14}$$

or

$$f_c = \frac{1}{\pi}\left(\frac{k_s^2 \kappa \ln 2}{4L}\right)^{1/4}. \tag{15}$$

Estimate (15), also plotted in Figures 2 and 3, is very accurate at high gains. One can also see that even at low gains it provides a closer and more conservative value to the actual bandwidth than any of Equations (10)–(12).

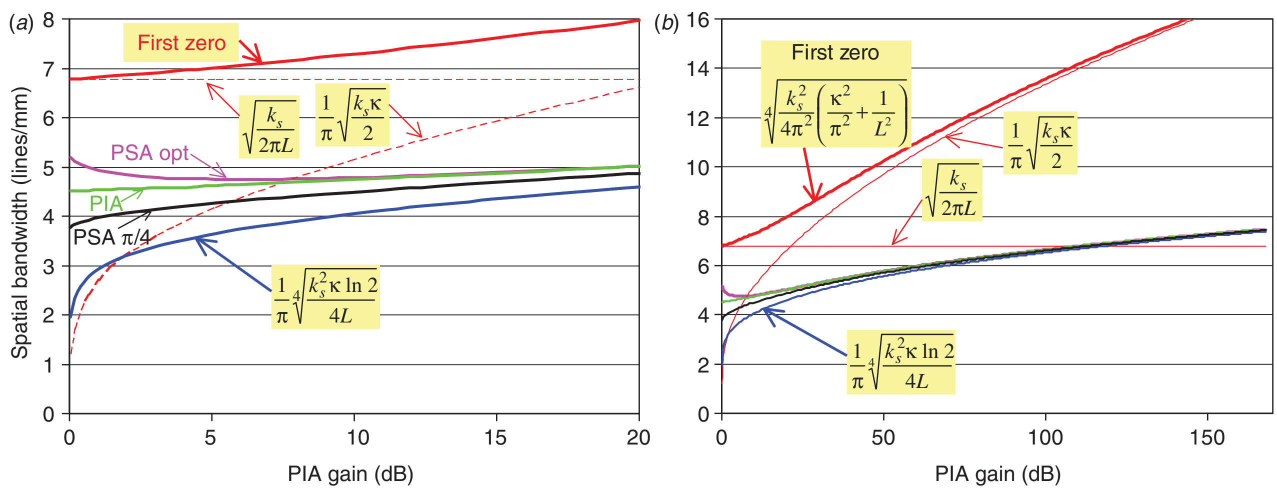

Figure 2. Spatial bandwidth $f_c = q_c/(2\pi)$ of a 25 mm long KTP-based OPA at 1550 nm signal wavelength, as a function of the PIA gain at zero spatial frequency. (*b*) Shows extended gain range for better view of the asymptotics. Labels 'PSA opt.', 'PIA', and 'PSA $\pi/4$' correspond to -3 dB bandwidths of PSA with optimum signal phase, PIA, and PSA with $\theta_s = \pi/4$ signal phase, respectively. Thick line at the top corresponds to the location of the first zero of $\nu(2\pi f)$. Thin and dashed lines are its asymptotes for low and high pump powers. The traditional estimate of spatial bandwidth corresponds to the low-power asymptote $[k_s/(2\pi L)]^{1/2}$ (horizontal thin and dashed line). $\Delta k = 0$ is assumed. (The color version of this figure is included in the online version of the journal.)

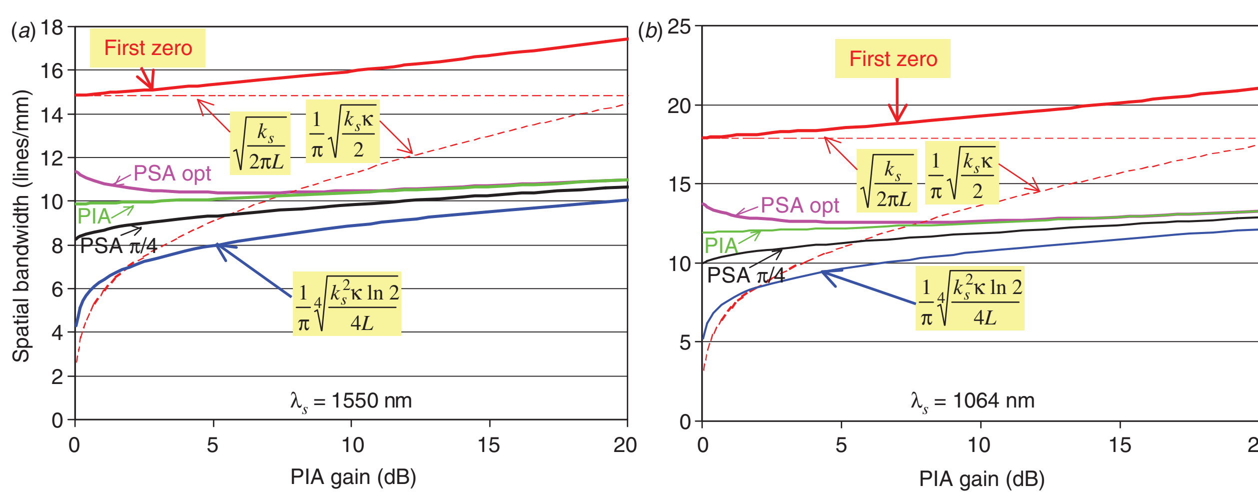

Figure 3. Comparison of spatial bandwidths $f_c = q_c/(2\pi)$ of a 5.21 mm long KTP-based OPA at 1550 nm (*a*) and 1064 nm (*b*) signal wavelengths, for $\Delta k = 0$. Line coding and other notations are the same as those in Figure 2. (The color version of this figure is included in the online version of the journal.)

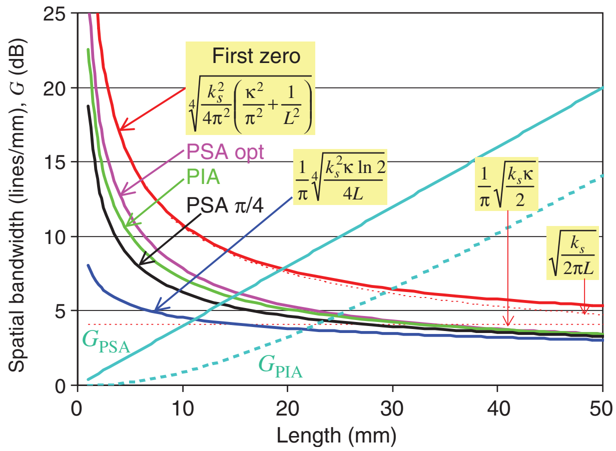

Figure 4. Spatial bandwidths $f_c = q_c/(2\pi)$ of a KTP-based OPA at 1550 nm as functions of crystal length L for a fixed pump power ($\kappa = 0.046\,\mathrm{mm}^{-1}$, which corresponds to 10 dB PSA gain for $L = 25$ mm). Line coding and other notations are the same as those in Figure 2. $\Delta k = 0$ is assumed. (The color version of this figure is included in the online version of the journal.)

The spatial bandwidth dependence on L is shown in Figure 4. Let us note that, for optimum signal phase, the phase-sensitive gain at large pump powers is also given by Equation (13), but without the factor of 1/4 in it. This indicates the applicability of Equation (15) to the phase-sensitive case as well.

Let us address the issue of the spatial bandwidth of the *phase-sensitive amplifier* (PSA) in greater detail. We note that, apart from the PIA-like spatial-frequency dependence of the gain originating from the magnitude of $\nu(q)$, another contributor to the gain is the signal phase θ_s that must be appropriate for the amplification. The maximum PSA gain

$$G_{\mathrm{PSA}}^{\mathrm{opt}} = [|\mu(q)| + |\nu(q)|]^2 = \left(G_{\mathrm{PIA}}^{1/2} + \left|(G_{\mathrm{PIA}} - 1)^{1/2}\right|\right)^2 \tag{16}$$

is achieved for optimum signal phase θ_s^{opt} from Equation (6) that is q-dependent and, therefore, may not be easily realizable. We can re-write Equation (6) as

$$2\theta_s^{\mathrm{opt}} - \pi/2 = \tan^{-1}\left[\frac{r}{(1-r^2)^{1/2}}\tanh\left[\kappa L(1-r^2)^{1/2}\right]\right] + \arg\left[\frac{1}{(1-r^2)^{1/2}}\sinh\left[\kappa L(1-r^2)^{1/2}\right]\right]. \tag{17}$$

In Equations (6) and (17) we assume that the function $\tan^{-1}$ produces no phase jumps when its argument jumps from $+\infty$ to $-\infty$, which in Equation (17) happens at points with $r^2 = 1 + [\pi(m+1/2)/(\kappa L)]^2$ and $m = 0, 1, 2, \ldots$. On the other hand, the second term in Equation (17) makes π phase jumps at $r^2 = 1 + [\pi(m+1)/(\kappa L)]^2$ for $m = 0, 1, 2, \ldots$ (sign of sinc function, i.e. polarity of ν, changes). The resulting piecewise-continuous optimum signal phase θ_s^{opt} for $\Delta k = 0$ is plotted in Figure 1 by a blue line. If, instead of the optimum phase, we choose a smooth function of spatial frequency without the phase jumps (i.e. without the second term in Equation (17)), which we will call an 'almost optimum phase', at the even-m turning points, the amplification in Figure 1 would be changing into an equal amount of de-amplification, yielding a smooth (but not optimum) PSA gain function. Even this 'almost optimum' phase is still q-dependent and not easily realizable.

Let us now consider two practically achievable cases. Assuming that $\Delta k = 0$ and that the input signal has a flat phase front with $\theta_s = \pi/4$ (i.e. optimum for zero spatial frequency), we obtain the PSA gain

$$G_{\mathrm{PSA}}^{\pi/4} = |\mu(q) - \mathrm{i}\nu(q)|^2 = \left|G_{\mathrm{PIA}}^{1/2} + \exp\left[\mathrm{i}(2\theta_s^{\mathrm{opt}} - \pi/2)\right](G_{\mathrm{PIA}} - 1)^{1/2}\right|^2. \tag{18}$$

Note that, since for high spatial frequencies $G_{\mathrm{PIA}} - 1$ is negative, the square root of it becomes a bipolar sinc function. Non-optimum PSA gain of Equation (18) is also plotted in Figure 1, which shows that, for the range of gains of interest, the non-optimum PSA spatial bandwidth is slightly narrower than the optimum one. The 3 dB PSA bandwidths of $(G_{\mathrm{PSA}} - 1)$ are plotted in Figures 2 to 4, which confirm this conclusion, but also show that the difference between optimum PSA, non-optimum PSA, and PIA bandwidths quickly disappears for gains ~10 dB and over. Also note that, for small values of κL, optimum signal phase θ_s^{opt} from Equations (6) and (17) is

$$\theta_s^{\mathrm{opt}} \approx \frac{\pi}{4} + \frac{\kappa L r}{2} = \frac{\pi}{4} + \frac{\Delta k L}{4} + \frac{q^2}{4k_s}L, \tag{19}$$

i.e. it is obtained by placing the focus of the image at $z_0 = L/2$ (middle of the crystal). PSA gain for such a converging beam is also plotted in Figure 1, and one can see that the difference between this and the optimum PSA gain is negligible, except for the areas of phase jumps, where this gain closely resembles that with 'almost optimum phase'. The difference between the actual optimum signal phase (6) and the approximate phase (19) is plotted in Figure 5 for several values of the PSA gain at zero spatial frequency and $\Delta k = 0$.

Finally, let us consider the consequences of the difference between the PSA gain with optimum phase and that with the 'almost optimum phase' (without phase jumps). The latter is described by a smooth function of spatial frequency, as opposed to the former. Since the amplitude gain represents the optical

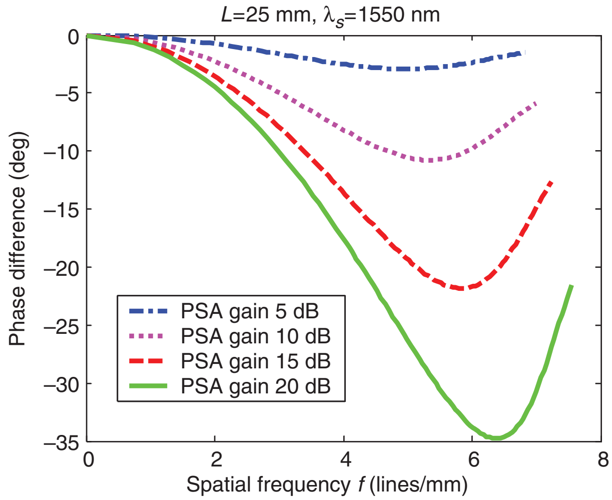

Figure 5. Difference between the actual optimum signal phase of Equation (6) and the approximate phase of Equation (19) for various values of the PSA gain at zero spatial frequency, assuming $\Delta k = 0$. The last point on each curve corresponds to the first zero of $\nu(2\pi f)$. (The color version of this figure is included in the online version of the journal.)

transfer function of the PSA, its inverse Fourier transform represents the point-spread function (PSF). Thus, the PSFs for the optimum and almost optimum cases are given by

$$\mathrm{PSF}^{\mathrm{optimum}}(\boldsymbol{\rho}) = \int \exp(\mathrm{i}\boldsymbol{q}\boldsymbol{\rho})[|\mu(q)| + |\nu(q)|]\frac{\mathrm{d}\boldsymbol{q}}{(2\pi)^2},$$
$$\mathrm{PSF}^{\mathrm{almostoptimum}}(\boldsymbol{\rho}) = \int \exp(\mathrm{i}\boldsymbol{q}\boldsymbol{\rho})[|\mu(q)| - \mathrm{i}\nu(q)]\frac{\mathrm{d}\boldsymbol{q}}{(2\pi)^2}. \tag{20}$$

(Here we have assumed that, since the input signal phase in Equation (20) contains at least the first term from the right-hand side of Equation (17), then a similar phase profile will be applied at the amplifier's output to eliminate the common phase of μ and ν, i.e. to bring the image into a focus.) Since both PSFs in Equation (20) contain the original $\delta(\boldsymbol{\rho})$-function of the unamplified point source plus the contribution of the PSA gain, for visualization purposes it is convenient to modify the PSFs by subtracting this δ-function. Such modified PSFs are shown in Figure 6. It is clear from this figure that the optimum gain function yields a narrower PSF because its rectification of the sinc function in the spatial-frequency domain produces a component of the PSF with a singularity at the origin. The smooth function of a PSA gain with 'almost optimum phase' yields a smooth PSF, and a similar PSF is expected for the PSA with image in the center of the crystal (phase given by Equation (19)).

To summarize, first of all we see that Equation (15) provides a better spatial bandwidth estimate than

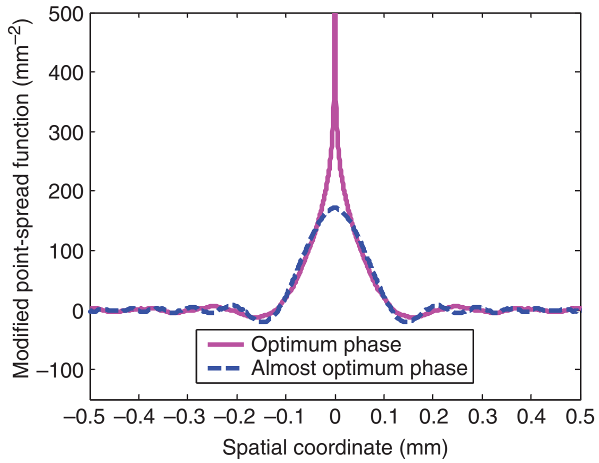

Figure 6. PSFs of Equation (20) modified by subtraction of $\delta(\boldsymbol{\rho})$-function, for a crystal with $L = 25$ mm, $\lambda_s = 1550$ nm, $\kappa L = 1.15$ (corresponding to 10 dB PSA gain at zero spatial frequency), and $\Delta k = 0$. 'Optimum phase' is given by Equation (6) with $\Delta k = 0$, and 'almost optimum phase' differs from it by the lack of $\pi/2$ phase jumps (last term in Equation (6)). (The color version of this figure is included in the online version of the journal.)

$q \sim (k_s/L)^{1/2}$ of Equation (11). Second, the differences between the PIA and PSA bandwidths (even with a flat input PSA phase) are not significant. If maximum PSA bandwidth is ultimately required, then the approximately parabolic shape of the optimum phase versus spatial frequency in Figure 1 suggests that simply placing the image focus at the location $z_0 = L/2$ (input beam converging into the middle of the crystal) solves the problem. Finally, the optimum PSA phase θ_s^{opt} with $\pi/2$ phase jumps of Equations (6) and (17) results in a somewhat narrower point-spread function compared to the other cases.

Acknowledgement

This work was supported by the DARPA Quantum Sensors Program.

References

[1] Lantz, E.; Devaux, F. *J. Sel. Top. Quant. Electron.* **2008,** *14,* 635–647.
[2] Kolobov, M. *Rev. Mod. Phys.* **1999,** *71,* 1539–1589.
[3] Choi, S.-K.; Vasilyev, M.; Kumar, P. *Phys. Rev. Lett.* **1999,** *83,* 1938–1941.
[4] Kumar, P.; Grigoryan, V.; Vasilyev, M., Noise-Free Amplification: Towards Quantum Laser Radar. In *The 14th Coherent Laser Radar Conference*, Snowmass, CO, July 8–13, 2007.
[5] Kolobov, M. *Quantum Imaging*; Springer Verlag: New York, 2007.
[6] Gavrielides, A.; Peterson, P.; Cardimona, D. *J. Appl. Phys.* **1987,** *62,* 2640–2645.